Research Article Adv. Mater. Lett. 2015, **6**(7), 585-591 Advanced Materials *Letters*

www.amlett.com, www.vbripress.com/aml, DOI: 10.5185/amlett.2015.5807 Published online by the VBRI press in 2015

Designing of MWCNT/ ferrofluid/ flyash multiphase composite as safeguard for electromagnetic radiation

Pradeep Sambyal[1], Avanish Pratap Singh[1], Meenakshi Verma[2], Ankit Gupta[3], Bhanu Pratap Singh[4], S.K. Dhawan[1*]

[1]*Polymeric & Soft Materials Section, CSIR-National Physical Laboratory, Dr. K. S. Krishnan Road, New Delhi 110 012, India*
[2]*Centre for Polymer Science & Engineering, Indian Institute of Technology, New Delhi 110012, India*
[3]*Delhi Institute of Tool Engineering, New Delhi 110 020, India*
[4]*Physics and Engineering of Carbon, CSIR-National Physical Laboratory, Dr. K. S. Krishnan Road, New Delhi 110 012, India*

[*]Corresponding author. Tel: (+91)-11-45609401; Fax :(+91)-11-25726938; E-mail: skdhawan@mail.nplindia.ernet.in

Received: 15 January 2015, Revised: 26 March 2015 and Accepted: 28 March 2015

ABSTRACT

Utilization of flyash which is produced at large scale in coal based thermal power plant is a challenge. In this regard, our investigation provides distinctive way of utilizing flyash for designing and preparing high-performance EMI shielding materials. Herein, we report synthesis and characterization of multiwalled carbon nanotubes (MWCNT) based multiphase composites. The multiphase composites were synthesized by in-situ co-precipitation with conductive filler (MWCNT) and magnetic filler (Ferro fluid). Scanning electron microscopy results confirm the presence of fly ash particles covered with Ferro fluid nanoparticles along with MWCNTs. Multiphase composites show total shielding effectiveness of 48 dB (>99.998 % attenuation) in the Ku-band (12.4–18 GHz) frequency range. The electromagnetic attributes, dielectric and permeability parameters have been calculated from the measured scattering parameters (S_{11}, S_{22}, S_{12}, S_{21}) using the Nicolson–Ross–Weir algorithm. The synthesized multiphase composites were characterized using XRD, FTIR, VSM and SEM. The results suggested that the MPC composites showed great potential as a radar absorbing material. Copyright © 2015 VBRI Press.

Keywords: EMI shielding; flyash; MWCNTs; ferrofluid.

Introduction

In the present world, electricity generation mainly depends on thermal power plants. These plants use coal as fuel that yields optimal heat to produce electricity. Flyash is the by-product of coal combustion. Every year a rough assessment of 600 million tons of flyash generated worldwide**[1]**. The utilization of flyash is still a challenge. From last decade, the requirement of environment friendly disposal of coal fly ash has amplified. The major part of flyash generated is disposed as filler in cement. Flyash is a solid waste material although it has certain beneficial properties, such as chemical inertness, thermal resistance, low density, strong filling ability, excellent fluidity, which makes it a unique material **[2-6]**. It is mainly composed of metal oxides (SiO_2, Al_2O_3, Fe_2O_3 and CaO) and has applications in many fields such as antistatic tiles, EMI shielding, geopolymers, cement substitutes and brick formation. Several attempts have been made for the utilization of flyash in various fields by different research groups e.g., Hardjito *et al.* **[7]** developed flyash based geopolymer concrete to reduce greenhouse emissions. Cao *et al.* **[8]** showed the efficient use of Flyash in photocatalytic removal on mercury in flue gas. Babajide et al. **[9]** demonstrated the use of coal fly ash as a catalyst in the production of biodiesel in which fly ash based catalyst was prepared using the wet impregnation procedure with different loadings of potassium. Flyash could be potentially used as electromagnetic interference (EMI) shielding material because it showed high dielectric constant **[10]**.

EMI shielding at higher frequency especially microwave radiation has become one of the serious concern to the society as it is not only affect the lifetime, performance of electronic gadgets but also have adverse effect on human beings **[11, 12]**. Therefore, EMI shielding materials are explored to guard the electronics and environment from polluting radiation coming out from computers and telecommunication equipment **[13, 14]**. In the past, several attempts have been made using various materials to design an effective shield that can completely absorb the unwanted radiation. In this regard, Singh *et al.* have developed polyaniline flyash composite for shielding application and observed a maximum shielding effectiveness (SE) of 32dB **[15]**. Chung and Cao reported 4 to 8 dB shielding effectiveness at 1 GHz by using flyash as an admixture in cement matrix **[16]**. Dou and coworkers measured the EMI shielding effectiveness properties of aluminum alloy–flyash composites in the frequency range of 30.0 kHz – 1.5 GHz and obtained a maximum SE of 102.5±0.1dB **[17]**.

From the previous studies, it is clearly proven that only flyash cannot be potentially used for EMI shielding. In general, the SE of a material depends on its dielectric properties, magnetic permeability, thickness and frequency. Therefore, to design a shield using flyash, a conducting filler (e.g. conducting polymers, carbon black, graphite, carbon fibers, carbon nanotubes, graphene) and a magnetic filler (Fe, Co, Ni, ferrites) should be employed in flyash based composite. Kiran *et al.* developed MWCNT based thermal grease with high thermal conductivity **[18]**. Srivastava *et al.* Show the possibility to reuse the spent CNTs for the removal of divalent metal ions in water and wastewater treatment. **[19]** Gouda *et al.* studied hardness properties of graphene and MWCNT based hybrid composite **[20].** Singh *et al.* prepared MWCNT based epoxy composites using solvent free industrial viable high energy homogenization technique and a significant improvement in the flexural strength and flexural modulus is achieved **[21]**. High conductivity, small diameter, high aspect ratio, low cost and superior mechanical properties make it a unique candidate to provide remarkable EMI Shielding **[22]**. In order to improve the magnetic permeability of the composite ferrofluid can be used due to its high magnetization, small size, and super paramagnetic behavior, environmental friendly and abundant natural supply **[23]**. The incorporation of ferrofluid enhances the microwave absorption by improving the equality of ε_r and μ_r. In the present investigation, flyash has been used to design an effective shield against electromagnetic radiation. MWCNT and ferrofluid have been incorporated to deliver the moderate conductivity and high permeability to the composite, respectively. The concentration of flyash in multiphase composite has also been optimized for their efficient utilization in EMI shielding. We expect our composite could act as an ideal shield against EM pollution and may be potentially used as a radar absorbing material.

Experimental

Materials

$FeCl_2.4H_2O$, $FeCl_3$ (Himedia, India) and aqueous ammonia solution, (Rankem Limited) were used for synthesis of ferrofluid. Toluene and ferrocene were procured from Rankem Limited. Fly ash is used after removing unburned carbon and other oxides. Aqueous solutions were prepared using double deionized water having specific resistivity of 10^6 Ω.cm. The other chemicals were of reagent grade and used as received.

Synthesis of multiwalled carbon nanotubes

MWCNTs were synthesized using chemical vapor deposition in quartz reactor by thermal decomposition of toluene in the presence of ferrocene as the catalyst. Experimental details are reported elsewhere **[24]**. The length of MWCNTs bundles was of ~350 μm and average diameter of ~26 nm **[25]**.

Synthesis of aqueous ferrofluid

Fe_3O_4 magnetite nanoparticles were synthesized by mixing $FeCl_2$ and $FeCl_3$ in the desired molar ratio **[26]**. A 4:1 molar ratio of 1.0 M $FeCl_3$ and 2.0 M $FeCl_2$ was mixed in an appropriate quantity of HCl and to this solution 1.0 M aqueous NH_3 solution was added, leading to the formation of brownish black precipitate, followed by the addition of surfactant which was 25% dextron in water, due to which the particles remained suspended in the liquid medium. The solution thus obtained exhibited spikes when placed in the proximity of a strong magnet and was used for further study.

In situ synthesis of MWCNT's/ aqueous ferrofluid/ fly ash composite

The multiphase composite of flyash, MWCNTs, and Fe_3O_4 nanoparticles were prepared by co-precipitation of $FeCl_2$ and $FeCl_3$ in the presence of flyash, MWCNTs as shown in **Fig. 1**. The detailed and systematic procedure is as follows: $FeCl_2$ and $FeCl_3$ in the desired molar ratio were mixed in an appropriate quantity of HCl. Then flyash and MWCNTs were mixed in the above solution and homogenized for 20 min and stirred. Then, 1.0 M aqueous NH_3 solution was added, leading to the formation of brownish black precipitate, followed by the addition of surfactant which was 25% dextron in water, due to which the particles remained suspended in the liquid medium. The product was obtained after filtration, followed by washing with distilled water until pH 7 was attained. In order to know the maximum amount of flyash loading, the different

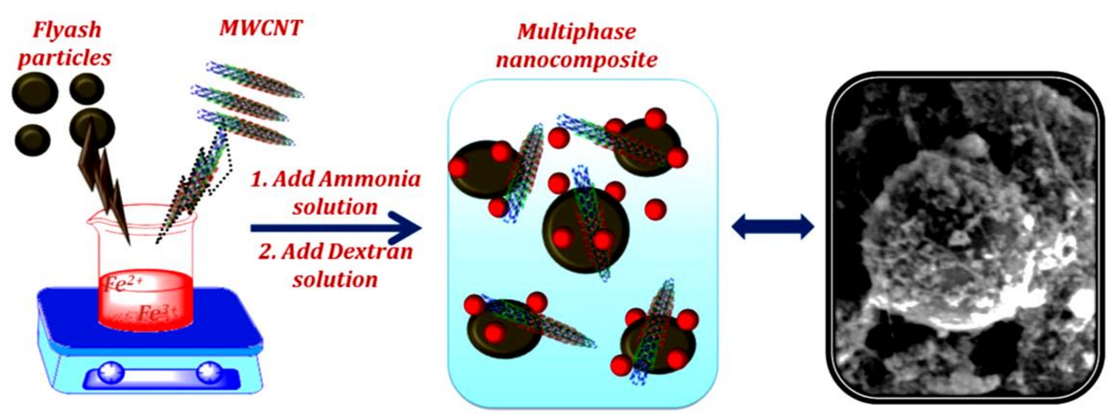

Fig. 1. Schematic representation of flyash particles surrounded with ferrofluid nanoparticles along with MWCNT'S by *in-situ* co-precipitation.

compositions of multiphase composite were synthesized by varying the flyash wt% ratios while keeping the other two constituents constant. The synthesized multiphase composites were abbreviated as MPC1 where MWCNTs, ferrofluid and fly ash are taken in 1:2:1 wt.% ratio, MPC2 where MWCNTs, ferrofluid and fly ash taken in 1:2:2 wt.% ratio, MPC3 where MWCNT, ferrofluid and fly ash are taken in 1:2:3 wt% ratio.

Characterization tools

The morphology of MPC composites have been examined using scanning electron microscope (SEM, Zeiss EVO MA-10). The SEM samples have been prepared by dispersing the powder in ethanol using ultra-sonication. The samples were gold sputtered before analysis. The element mapping distribution of the samples were analyzed by energy dispersive X-ray spectroscopy which is associated with SEM. X-ray diffraction (XRD) analysis was carried out on D8 Advance XRD (Bruker) using CuKα radiation (λ= 1.54Å) in the scattering range (2θ) of 10°-80°. FTIR spectra have been recorded on Nicolet 5700 in transmission mode in the wave number range 400-4000 cm^{-1}.Thermogravimetric analyzer (Mettler Toledo TGA/SDTA851e) has been used to measure the thermal stability of the material under inert atmosphere (flowing N_2 gas) in the temperature range 25-900°C (for detail see supporting material information). The magnetic measurements of MPC composites were carried out using the vibrating sample magnetometer (VSM), Model 7304, Lakeshore Cryotronics Inc. The electrical conductivity of MPC composites have been measured at room temperature by a standard four-probe technique using Keithley semiconductor characterization system 4200. EMI shielding and dielectric measurements have been carried out using Agilent E8362B vector network analyzer in the 12.4-18 GHz (Ku-band) microwave range,(for detail see supporting material information) . Powder samples have been compressed in the form of rectangular pellets (~2.5mm thickness) and inserted in copper sample holder connected between the wave-guide flanges of network analyzer.

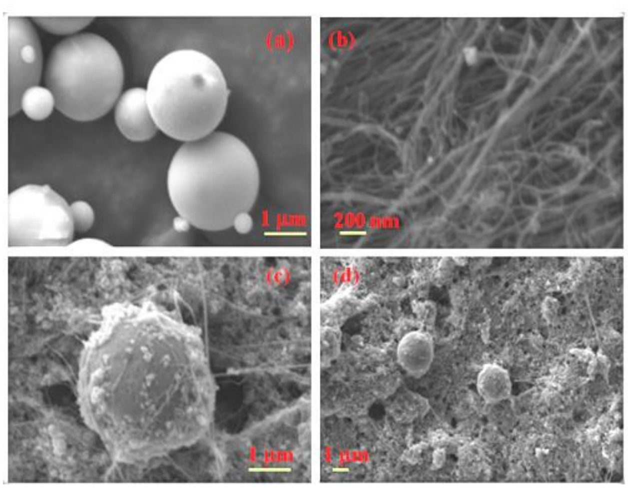

Fig. 2. SEM images of (a) flyash micro-particles (b) MWCNT (c, d) MPC3 composite, showing flyash particle coated with ferrofluid particle along MWCNTs.

Results and discussion

Surface morphology and microstructural analysis

SEM was carried out to study the distribution of flyash and MWCNT in the ferrofluid matrix. **Fig. 2 (a)** shows the SEM image of flyash particles up to a few micrometer in diameter, since flyash is composed of different oxides like SiO_2, Al_2O_3, CaO, K_2O therefore the different size spheres (diameter ranges from 50 nm - 5 µm) were seen in the SEM images. **Fig. 2(b)** shows high aspect ratio MWCNTs [10]. SEM micrograph of MPC3 composites reveals that flyash particles are partially covered with ferrofluid nanoparticles along with MWCNT as appear in **Fig. 2 (c)** and **Fig. 2 (d)**.

The presence of conducting and the dielectric nanoparticles in the ferrofluid matrix is helpful for the proper impedance matching, which is necessary for enhancing the absorption of the EM wave. **Fig. 3 (a)** TEM image of multiphase composite (MPC1) shows uniform distributed MWCNT, flyash particles covered with Ferrofluid nanoparticles. The arrow shows the MWCNT and micro-flyash particle covered with ferrofluid is encircled. **Fig. 3 (b)** shows EDS pattern of flyash, the approximate percentage of the constituents of flyash like SiO_2, Al_2O_3, K_2O, and CaO etc. while **Fig. 3 (c)** shows the EDS pattern of multiphase composites (MPC1), there is a increase in the content of Fe & Carbon weight % in multiphase composites as compare to neat flyash.

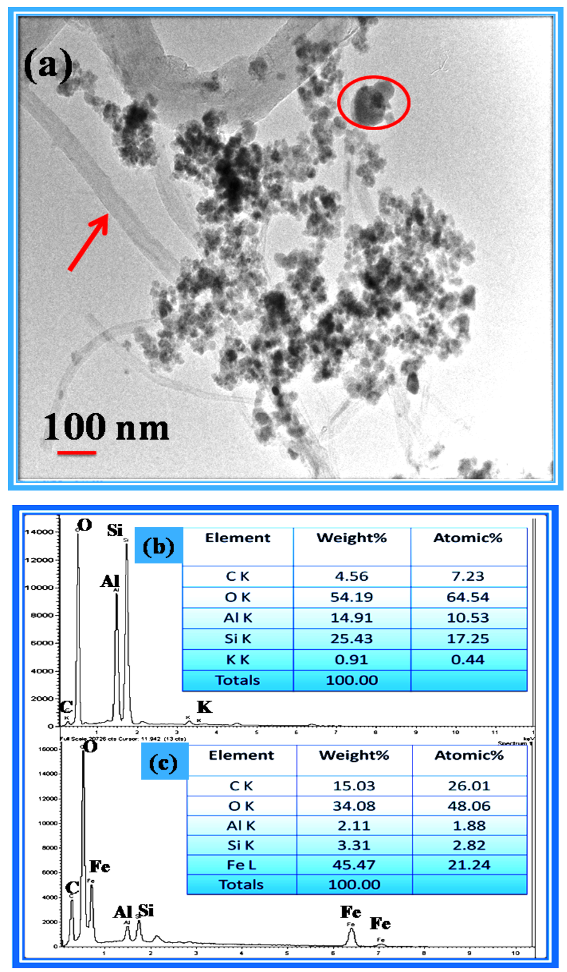

Fig. 3. (a) TEM image of MPC1 composite, EDS pattern of (b) flyash micro-particles and (c) MPC1 composite.

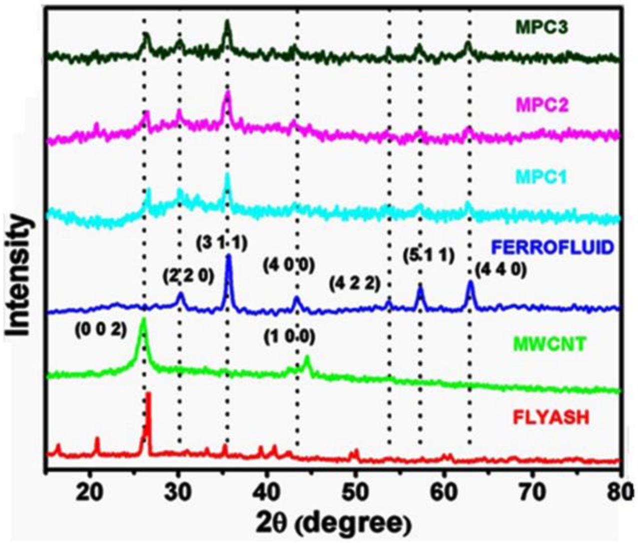

Fig. 4. XRD pattern of fly ash, MWCNTs, ferrofluid, MPC1, MPC2 and MPC3.

Structural analysis

Fig. 4 shows the XRD patterns of pure MWCNT, flyash, ferrofluid and multiphase composites i.e.MPC1, MPC2, MPC3. Flyash shows the characteristics peaks at 2θ = 26.68° (d = 3.3409 Å), 33.36° (d = 2.6931 Å), 35.22° (d = 2.5433 Å), 39.88° (d = 2.2057 Å), 42.46° (d = 2.1196 Å), 54.04° (d = 1.6955 Å), 60.68° (d = 1.5249 Å) and 64.60° (d = 1.4435 Å) **[27]**. The XRD patterns of MWCNT shows reflection peaks at 2θ values of 26.5°, 42.64°,corresponding to (0 0 2) (1 0 0), sets of diffraction planes, respectively **[28]**. XRD pattern of Fe_3O_4 shows a main peaks at 2θ values of 30.16° (d = 2.96 Å), 35.53° (d = 2.53 Å), 43.18° (d = 2.09 Å), 57.11° (d = 1.61 Å) and 62.71° (d = 1.48 Å) which corresponds to the (2 2 0), (3 1 1), (4 0 0), (5 1 1) and (4 4 0) reflection planes which matches with the standard XRD pattern of Fe_3O_4 (Powder Diffraction File, JCPDS card No. 88-0315). The composites show the characteristics peaks of MWCNT, flyash and ferrofluid, their intensity increases monotonically with increase in the content. It is seen that all the detectable peaks of flyash and ferrofluid are well retained and no other peak is observed indicating that no chemical reaction occurred between MWCNT, ferrofluid and flyash. These observations indicate that there is no change in the morphology of flyash, although it was coated by ferrofluid particles.

The crystalline size of particles can be calculated by using Debye Scherer's formula:

$$D = k\lambda / \beta Cos\theta$$

where k is the Scherrer constant and equals 0.89, which is governed by several factors, including the Miller index of the reflecting plane and the shape of the crystal. λ is the X-ray wavelength, θ is the angle of the Bragg diffraction, and β is the full width at half-maximum of the sample. D is crystalline size for individual peak. The average size of Fe_3O_4 particles was calculated using above equation and estimated as 10.6 nm for pure Fe_3O_4 and 11.3 nm for Fe_3O_4 nanoparticles presented in multiphase composites.

FTIR spectroscopy

Fig. 5 shows FTIR spectra of pure Fly ash, ferrofluid, and its composites. Fly ash spectra show a wide band which is a characteristic of the internal vibrations in silicates. The band corresponding to asymmetric stretching vibration of T-O (T = Al, Si) in the fly ash appears at 1083.90 cm^{-1}. Bands at 457.45 cm^{-1} are assigned to T-O bending vibrations. The bands at 780-795 cm^{-1} are attributed to the presence of quartz in the fly ash. The band at 550-560 cm^{-1} corresponds to the mullite present in the fly ash. **[29]** Ferrofluid spectra show bending vibration of Fe-O, O-H at 582 cm^{-1} and 1620 cm^{-1} .The broad band observed around 3380-3430 cm^{-1} is due to the O-H stretching vibrations. These results are in good agreement with the previous spectroscopic characterization of Ferrofluid **[30]**. However, in case of composites, shows the characteristics band of ferrofluid and flyash indicating that flyash particles covered with ferrofluid also confirmed by SEM image (**Fig. 2c**). There is slight shifting and broadening of characteristics bands was observed which indicates the presence of physical interaction between MWCNT, ferrofluid and flyash. Absence of any new vibration band suggests a Vander Wall's kind of interaction without any chemical origin.

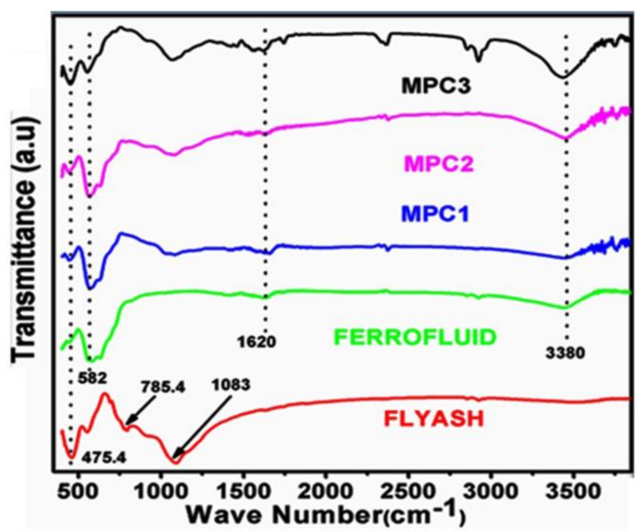

Fig. 5. FTIR spectra of fly ash, Ferrofluid, MPC1, MPC2 and MPC3.

Dielectric and magnetic properties of multiphase composites

Fig. 6 (a) shows the real and imaginary part of complex permittivity and permeability for sample MPC3, as a function of frequency. The real part of permittivity (ε') symbolizes the intensity of polarization and it is a direct measure of the electrical energy storage ability of a material and permittivity loss represents the energy loss during the activation by an EM wave. The value of ε' fluctuates between 148 and 190. The value of ε'' is lower than ε' and it varies from 74 to 93 with fluctuations in 12.4 to 18 GHz. The high value of ε'' for multiphase composite exhibits high dielectric losses. Interestingly, there are two humps observed in dielectric loss which proposed that the two main phenomena's are responsible for dielectric losses. These may be interfacial polarization between flyash particles and MWCNTs, ferrofluid and MWCNTs and high anisotropy energy of the multiphase composite. Anisotropy energy of the small size materials like ferrofluid nanoparticles would be higher due to surface anisotropic field due to the small size effect **[23]**. The higher anisotropy energy also contributes in the enhancement of the microwave absorption. The real part of permeability (μ') varies from 1.17 to 0.63 while the imaginary part (μ'') i.e. permeability loss varies from 0.45 to 0.18. The fluctuations in the permeability curves reveals natural resonances in the multiphase composite which can be ascribed to small size of Fe_3O_4 nanoparticles. The both dielectric and magnetic losses share the improved shielding performance of the as-synthesized multiphase composites.

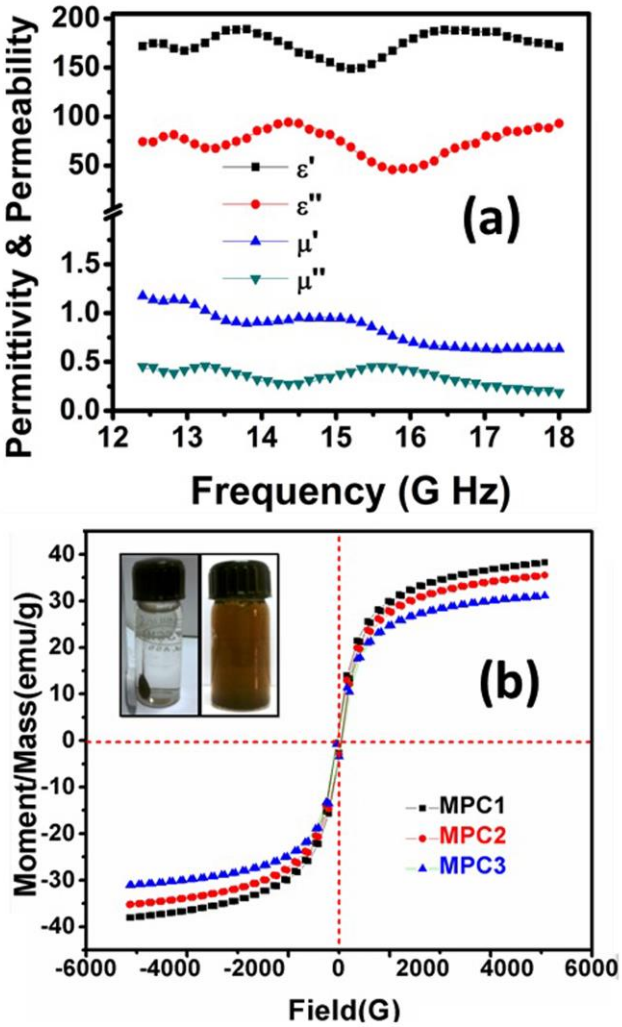

Fig. 6. (a) Shows frequency dependence of the real parts and imaginary parts of the complex permittivity and permeability of Multiphase composites, and (b) represents vibrating sample magnetometer plots of the Multiphase composites while Inset image shows the magnetic behavior of multiphase composite in presence and absence of bar magnet.

To further understand the magnetic behavior of the multiphase composites, the magnetic properties of the MWCNT/ferrofluid/flyash composites have been explored using the M–H curve (**Fig. 6b**). When MWCNTs are incorporated in the ferrofluid matrix with flyash in different weight ratio (i.e. 1:2:1 MPC1), the magnetization saturation (Ms) value has been found 38.26 emug^{-1} at an external field of 5 kOe having small value of coercivity and negligible retentivity with no hysteresis loop, representing the super paramagnetic nature. However, on changing the weight composition of MWCNT/ferrofluid/flyash to 1:2:2, the Ms value has been decreased from 38.26 to 35.50 emug^{-1}, keeping the external applied field at 5 kOe. Ms value further decrease to 31.10 emug^{-1} on changing the weight composition of MWCNT/ferrofluid/flyash to 1:2:3.In all the cases very small coercivity is observed with negligible retentivity which indicates the ferromagnetic nature. Decrease in Ms value is due to increase in the content of dielectric material in MPC composite matrix.

EMI shielding Efficiencies of multiphase composites

From the basic theory of EMI shielding **[14, 23, 31]**, an ideal microwave shield must be a multiphase composite which contains the optimum concentration of electrically conducting material, dielectric filler and magnetic material. Along with this, physical geometry also plays crucial role in improving the SE. Moderate conductivity (10^{-4} to 10^{-1} S/cm) of the composite improves SE in two ways, first, incident EM wave reflected from the front face of conducting shield because interaction of electric vector with mobile charge carriers present on conducting surface resulted in ohmic losses (heat). Second, for materials consisting of a high concentration of charge carriers (i.e., with a high conductivity), polarization due to the migration of charge carriers to form space charges at interfaces or grain boundaries becomes important. This space charge polarization enhances the polarization effect **[23, 32]**.

Being highly magnetic, conductive and high dielectric, flyash/ferrofluid/MWCNTs composites are an ideal material for EMI shielding to block polluting radiation in electronic gadgets. Certainly, MWCNTs and ferrofluid are counted for unprecedented EMI SE of flyash. The multiphase composites delivered exceptional EMI SE as high as about 48 dB at 25 wt% loading of flyash (**Fig. 7a**), The SE decreased with increasing flyash loading in multiphase composite and reached a value of 38 dB at 50 wt% loading which is more than sufficient SE value required for commercial applications.

Table 1. The dc electrical conductivity and shielding effectiveness of multiphase composites.

Sample Name	Conductivity (S/cm^{-1})	Shielding Effectiveness (dB)		
		SE_A	SE_R	SE_T
MPC1	38.56	~41	7.19	~48
MPC2	22.10	~36	8.22	~44
MPC3	10.49	~30	7.35	~37

The decreased in SE value with higher flyash loading can be attributed to two reasons, first incorporation of flyash leads to significant decrease in conductivity of multiphase composite as shown in **Table 1**, second higher wt % of dielectric filler flyash raises the permittivity and lowering the equality of impedance matching i.e. $\varepsilon_r > \mu_r$.

Fig. 7b shows the variation of SE due to absorption (SE_{Abs}) and due to reflection (SE_{Ref}) over the Ku band frequency range. Both SE_{Abs} and SE_{Ref} are collectively contributing to the total effective SE. The value of SE_{Abs} for MPC1, MPC2 and MPC3 were found to be ~40, ~36 and ~30 dB, respectively while the value of SE_{Ref} for all the composites is nearly same ~7dB. This is similar to the previous results i.e. SE_{Abs} becomes more dominant as compared to the SE_{Ref} in the microwave range. From these results, it is concluded that total SE is mainly dominated by SE_{Abs} while the SE_{Ref} is constant. Bare flyash shows a SE value of ~2.5 dB in Ku band (see supporting information). Therefore, it is worthy to notice that, total SE for all multiphase composites is multifold of bare flyash. For a given flyash content, all multiphase composites showed little fluctuation over the entire frequency range studied. The above observation is associated with three exceptional features of the multiphase composites: explicitly, (i) the presence of dielectric constituents in flyash contributed positively to shielding the electromagnetic waves (ii) ferrofluid nanoparticles act as tiny dipoles which get polarized by the activation of EM field and result in better microwave absorption and (iii) the highly conductive MWCNT/ferrofluid/flyash multiphase composites had high charge storage capacities, capable of absorbing the incidental EM waves by polarization in the electric field. Besides these phenomena's, when EM waves incident on the material, ionic, electronic, orientational and space charge polarization occurs. The contribution to the space charge polarization appears due to the heterogeneous property of the material **[14]**. From the all above, the result promises that these composites could be potentially used as a kind of radar absorbing material.

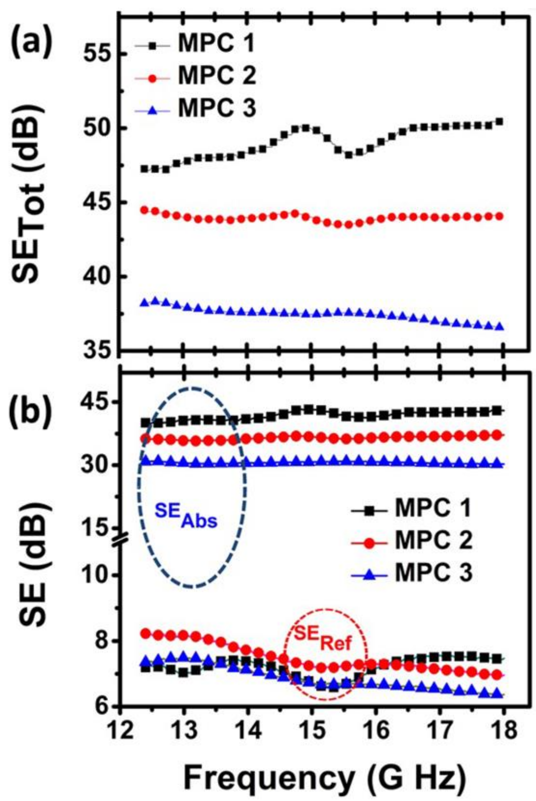

Fig. 7. (a) EMI SE (b) SE_A and SE_R of multiphase composite as a function of frequency.

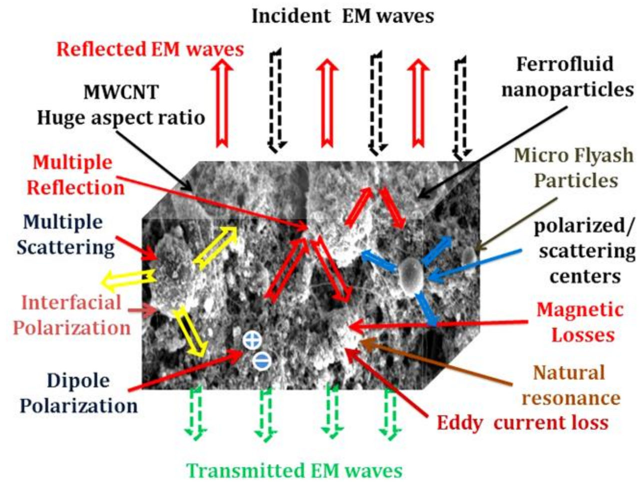

Fig. 8. Possible shielding mechanism of multiphase composites.

Conclusion

Multiphase composites consists of flyash, ferrofluid and MWCNTs have been prepared for efficient microwave shielding with different composition by utilizing the fly ash a waste material from various industries. This composition has been optimized and found MPC1 (1:2:1) better microwave shielding material where 48 dB of EMI shielding achieved in 12.4-18 GHz frequency (Ku band). The shielding effectiveness was strongly dependent on dielectric loss and volume fraction of in FA matrix. The high value of shielding effectiveness demonstrates the potential of these advanced multiphase composite as futuristic microwave shielding materials.

Acknowledgements

The authors gratefully acknowledge Prof. R. C. Budhani, Director, CSIR-NPL and New Delhi, India for constant encouragement and support. The work is supported by Ministry of Environment & Forests, Government of India network (GAP-11432). The authors thank Dr. N. Vijayan, Mr. K. N. Sood and Dr. R. K. Kotnala for recording XRD pattern, SEM micrograph and VSM.

Reference

1. Yao, Z. T.; Xia, M. S.; Ye, Y.; Zhang, L.;*Journal of Hazardous Materials*, **2009,** *170* (2–3), 639.
   DOI: 10.1016/j.jhazmat.2009.05.018
2. Ngu, L.-n.; Wu, H.; Zhang, D.-k.;*Energy & Fuels*, **2007,** *21* (6), 3437.
   DOI: 10.1021/ef700340k
3. Wang, W.; Li, Q.; Wang, B.; Xu, X.-T.; Zhai, J.-P.; *Materials Chemistry and Physics*, **2012,** *135* (2), 1077.
   DOI: 10.1016/j.matchemphys.2012.06.020
4. Lu, J.; Xu, F.; Wang, D.; Huang, J.; Cai, W.; j*ournal of Hazardous Materials*, **2009,** *165* (1), 120.
   DOI: 10.1016/j.jhazmat.2008.09.090
5. Wang, B.; Li, Q.; Wang, W.; Li, Y.; Zhai, J.;*Applied Surface Science*, **2011,** *257* (8), 3473.
   DOI: 10.1016/j.apsusc.2010.11.050
6. Shao, L.; Qiu, J.; Liu, M.; Feng, H.; Zhang, G.; Qin, L.;*Synthetic Metals* ,**2010,** *160* (1), 143.
   DOI: 10.1016/j.synthmet.2009.10.022
7. Hardjito, D.; Wallah, S. E.; Sumajouw, D. M.; Rangan, B. V.; *ACI materials journal*, **2004,** *101* (6).
   DOI: 10.14359/13485
8. Cao, Y. X.; Fang, J. H.; Wu, J.; Li, X.; Zhang, C.; Li, C. E.; Hu, C. Z.; Li, S.;*Advanced Materials Research*, **2014,** *864*, 1546.
   DOI: 10.4028/www.scientific.net/AMR.864-867.1546
9. Babajide, O.; Petrik, L.; Musyoka, N.; Amigun, B.; Ameer, F.;*Petroleum & Coal*, **2010,** *52* (4), 261.
   DOI: 10566/574

10. Raghavendra, S. C.; Raibagkar, R. L.; Kulkarni, A. B.; *Bull Mater Sci,* **2002,** *25* (1), 37.
DOI: 10.1007/BF02704592
11. Gooch, J. W.; Daher, J. K.;. Springer: 2010.
12. Chen, Z.; Xu, C.; Ma, C.; Ren, W.; Cheng, H.-M.;*Advanced Material,*. **2013,** *25* (9), 1296.
DOI: 10.1002/adma.201204196
13. Song, W.-L.; Cao, M.-S.; Lu, M.-M.; Bi, S.; Wang, C.-Y.; Liu, J.; Yuan, J.; Fan, L.-Z.; *Carbon,* **2014,** *66* (0), 67.
DOI: 10.1016/j.carbon.2013.08.043
14. Sambyal, P.; Singh, A. P.; Verma, M.; Farukh, M.; Singh, B. P.; Dhawan, S. K.;R*SC Advances,* **2014,** *4* (24), 12614.
DOI: 10.1039/C3RA46479B
15. Singh, A. P.; S., A. K.; Chandra, A.; Dhawan, S. K.; *AIP Advances,* **2011,** *1* (2),022147.
DOI: 10.1063/1.3608052
16. Cao, J.; Chung, D.;*Cement and Concrete Research,* **2004,** *34* (10), 1889.
DOI: 10.1016/j.cemconres.2004.02.003
17. Dou, Z.; Wu, G.; Huang, X.; Sun, D.; Jiang, L.;*Applied Science and Manufacturing,* **2007,** *38* (1), 186.
DOI: 10.1016/j.compositesa.2006.01.015
18. Sashi Kiran C.; K. K. Nanda.;Advanced materials letters,2013,1,22.
DOI: 10.5185/amlett.2013.icnano.327
19. Saksham Srivastava; ; Advanced materials letters,2013,4(1),2
DOI: 10.5185/amlett.2013.icnano.110
20. P.S. Shivakumar Gouda.; Raghavendra Kulkarni.; S.N. Kurbet.; Dayananda Jawali; *Adv. Mat. Lett.*, 2013,4(4),261
DOI: 10.5185/amlett.2012.9419
21. Singh. B.P.; Choudhary, V.; Teotia S.; Gupta T. K.; Singh, V.N.; Dhakate, S.R.; Mathur, R.B. *Adv. Mat. Lett.* **2015**, *6(2)*, 104.
DOI: 10.5185/amlett.2015.5612
22. Gupta, T. K.; Singh, B. P.; Dhakate, S. R.; Singh, V.; Mathur, R. B.;*J. Mater. Chem. A* **2013**,**1**(32), 9138.
DOI: 10.1039/C3TA11611E
23. Singh, A. P.; Mishra, M.; Sambyal, P.; Gupta, B. K.; Singh, B. P.; Chandra, A.; Dhawan, S. K.; *Journal of Materials Chemistry A,* **2014,** *2* (10), 3581.
DOI: 10.1039/C3TA14212D
24. Mathur, R. B.; Chatterjee, S.; Singh, B. P.; *Composites Science and Technology,* **2008,** *68* (7–8), 1608.
DOI: 10.1016/j.compscitech.2008.02.020
25. Singh, B. P.; Saini, K.; Choudhary, V.; Teotia, S.; Pande, S.; Saini, P.; Mathur, R. B.;*J Nanopart Res,* **2013,** *16* (1),1.
DOI: 10.1007/s11051-013-2161-9
26. Singh, A. P.; Mishra, M.; Chandra, A.; Dhawan, S.; *Nanotechnology* ,**2011,** *22* (46), 465701.
DOI: 10.1088/0957-4484/22/46/465701
27. Jha, B.; Koshy, N.; Singh, D. N.;*Frontiers of Environmental Science & Engineering*,1.
DOI: 10.1007/s11783-014-0630-8
28. Singh, A. P.; Gupta, B. K.; Mishra, M.; Govind; Chandra, A.; Mathur, R. B.; Dhawan, S. K.; *Carbon* ,**2013,** *56* (0),86.
DOI: 10.1016/j.carbon.2012.12.081
29. Fernández-Jiménez, A.; Palomo, A.; *Microporous and mesoporous materials,* **2005,** *86* (1), 207.
DOI: 10.1016/j.micromeso.2005.05.057
30. Seckin, T.; Vural, S.; Köytepe, S.; *Polym. Bull.*,**2010,** *64* (2), 115
DOI: 10.1007/s00289-009-0135-y
31. Ebrahimi, F.; *Nanocomposites - New Trends and Development*., InTech: 2012.
DOI: 10.5772/33892. Das, C. K.; Mandal, A.;Nanocomposites., **2012,** *1* (1), 43.
DOI: 10.5539/jmsr.v1n1p45

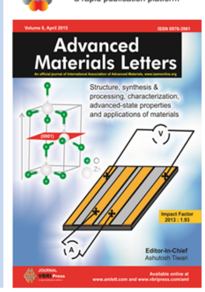

Supporting information

Fig. S1 shows the thermal stability of MWCNT/flyash/ferrofluid composites.MPC1 shows two step weight loss behavior .The first stage attributes to loss of residual moisture and solvents. The MPC composite shows thermal stability upto 518 ^{o}C, 535 ^{o}C and 568 ^{o}C for different concentrations. The TGA data shows that MPC3 with higher loading of flyash shows highest thermal stability over other composites.

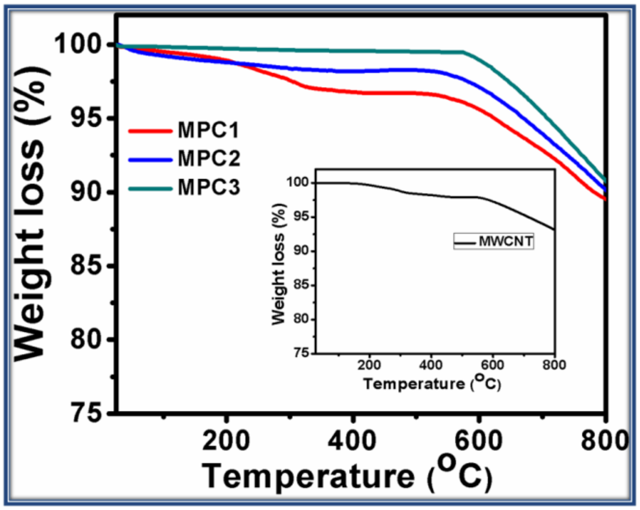

Fig. S1. Thermogravimetric analysis of MPC composites and MWCNT

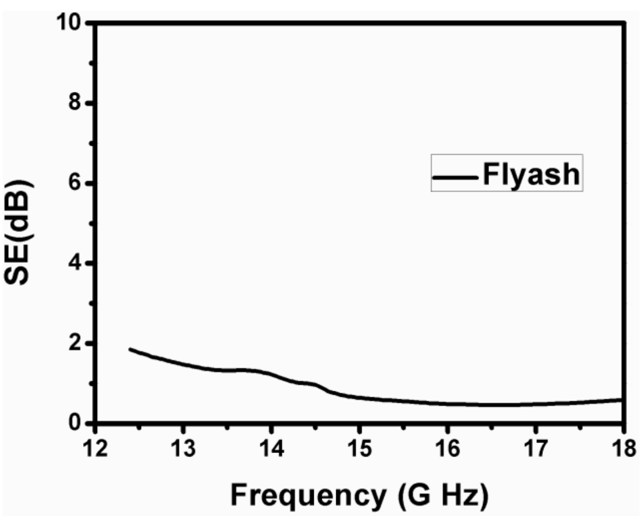

Fig. S2. Variation of EMI SE with frequency for bare flyash.

Set up for shielding measurement

Electromagnetic shielding performance, dielectric and permeability properties of the composites were carried out on an Agilent E8362B Vector Network Analyzer in a microwave range of12.4-18 GHz (Ku-band). Powder samples were compressed in the form of rectangular pellets and inserted in the grove of dimension 15.9 x 7.90 x 3 mm^3 copper sample holder connected between the wave-guide flanges of vector network analyzer. The set up for measurement is shown in **Fig. S3**.

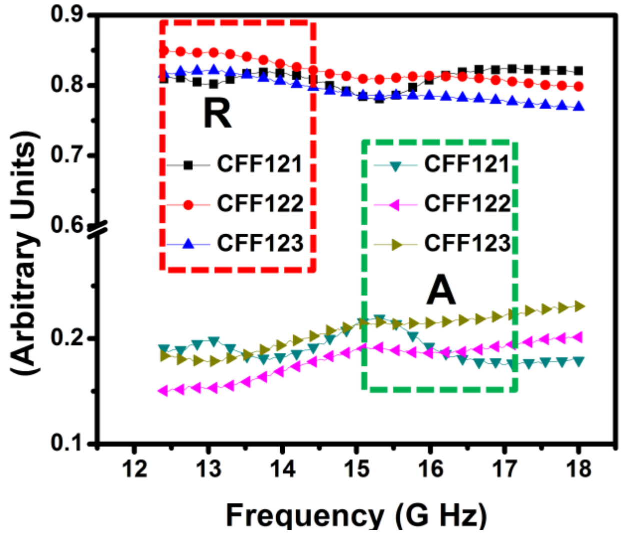

Fig. S2. Variation of absorptivity (A) and reflectivity (R) with frequency.

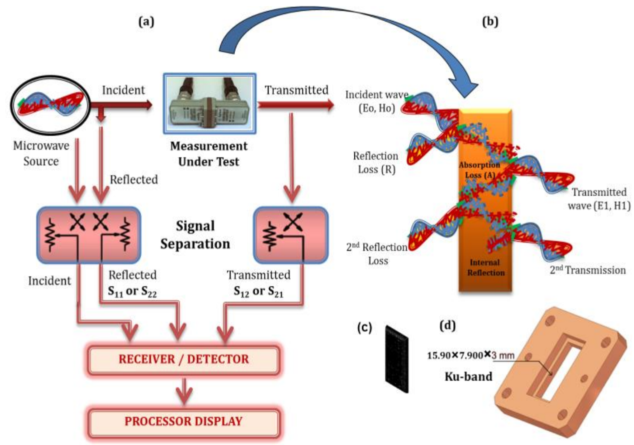

Fig. S3. (a) Schematic for measurements of S parameters (S_{11}, S_{22}, $S_{12}$and S_{21}) using the vector network analyzer (b) Interaction of EM waves with the sample under test, (c) Sample is compressed in pallet form of desired thickness (d) Sample holder of Ku-band.

The S parameters S_{11} (S_{22}), S_{12} (S_{21}) of the MPC composites were measured by vector network analyzer (VNA E8263B Agilent Technologies) in the frequency range of 12.4 – 18 GHz (Ku band) using two port measurement techniques. The powder samples were compressed into rectangular pellets with dimensions 15.9 X 7.9 mm^2 and inserted in a copper sample holder connected between the waveguide flanges of a network analyzer. The power coefficients, transmission coefficient (T) and reflection coefficient (R) were calculated by the equations

$$T = \left|\frac{E_T}{E_I}\right|^2 = |S_{21}|^2 = |S_{12}|^2 \quad (1)$$

$$R = \left|\frac{E_R}{E_I}\right|^2 = |S_{11}|^2 = |S_{22}|^2 \quad (2)$$

And absorption coefficient was calculated from the relation of

$$(A) = 1 - R - T$$

Here, it is noted that the absorption coefficient is given with respect to the power of the incident electromagnetic wave.

If the effect of multiple reflections between both interfaces of the material is negligible, then the relative intensity of the effectively incident electromagnetic wave inside the material after reflection is based on the quantity $(1 - R)$. Therefore, the effective absorbance (A_{eff}) can be described as $A_{eff} = A / (1 – R)$ with respect to the power of the effective incident electromagnetic wave inside the shielding material. Absorption efficiency (AE) was obtained using the relation of AE=A/(1-R)×100%. The electromagnetic attributes, dielectric and permeability parameters have been calculated from the measured S parameters using the Nicolson–Ross–Weir algorithm (A. Nicolson and G. Ross, Instrumentation and Measurement, IEEE Transactions on, 1970, 19, 377-382.)

For a shielding material, total SE = $SE_R + SE_A + SE_M$, where SE_R, SE_A, and SE_M are shielding effectiveness due to reflection, absorption, and multiple reflections, respectively. The EMI SE of a material can be written mathematically as

$$SE(dB) = -10log\left(\frac{P_T}{P_I}\right) = -20\log\left(\frac{E_T}{E_I}\right) = -20\log\left(\frac{B_T}{B_I}\right) \quad (3)$$

Where symbol P, E and B stands for power, Electric and magnetic field intensity. The subscript $_T$ and $_I$ used for the transmitted and incident wave on the shield, respectively. The correction term SE_M can be ignored in all practical application when SE >10 dB as

$$SE\ (dB) = SE_R\,(dB) + SE_A\,(dB) \quad (4)$$

In equation 4, the first term is related to the reflection of the electromagnetic wave and contributes as the SE due to reflection. The second term expresses the loss due to the absorption of the wave when it passes through the shielding material. Dependence of SE on dielectric properties & magnetic properties can be expressed as

$$SE_R\ (dB) \approx 10\log\left(\sigma_{ac}/(16\omega\varepsilon_0\mu_{r)}\right) \quad (5)$$

And

$$SE_A\,(dB) = 20\left\{\frac{t}{\delta}\right\}\log e = 20\,t\sqrt{\frac{\mu_r\omega\sigma_{ac}}{2}} = 8.68\left(\frac{t}{\delta}\right) \quad (6)$$

Where σ_{ac} depends on the dielectric properties ($\sigma_{ac} = \omega\varepsilon_0\varepsilon''$) of the material, ω is the angular frequency ($\omega = 2\pi f$), ε_0 is the free space permittivity, and μ_r is the relative magnetic permeability of the sample.

It is convenient to express SE_R and SE_A in terms of the reflectance −10 log (1 – R) and effective absorbance −10 log $(1 – A_{eff})$ in decibel (dB), respectively

$$SE_R = -10\log\,(1 - R) \quad (7)$$

And

$$SE_A = -10\log\left(1 - A_{eff}\right) = -10\log\left(\frac{T}{1-R}\right) \quad (8)$$

Using these mathematical expressions we can calculate shielding performance of the composite.